Electron transport through a single nanocrystalline silicon quantum dot between nanogap electrodes

T. Sawada, T. Kodera,[a] and S. Oda[b]
Department of Physical Electronics and Quantum Nanoelectronics Research Center, Tokyo Institute of Technology, 2-12-1-S9-11 Ookayama, Meguro, Tokyo 152-8552, Japan

(Received 7 September 2016; accepted 6 November 2016; published online 21 November 2016)

We experimentally study the electron transport through a single nanocrystalline silicon quantum dot between the nanogap electrodes. We fabricate the device by depositing a nanocrystal into an ~10-nm gap using a very high frequency plasma cell. The Coulomb diamond size depends on the number of electrons at 4.5 K, which indicates that even–odd shell filling occurs. The charging energy is estimated to be ~11 meV, which is consistent with the size of the silicon nanocrystal. The perpendicular magnetic field dependence of the Coulomb diamonds demonstrates the Zeeman splitting as well as orbital energy evolution. *Published by AIP Publishing.*
[http://dx.doi.org/10.1063/1.4968008]

Recently, silicon quantum dots (Si QDs) have been actively studied owing to their potential to realize the quantum information devices.[1–12] Long electron spin coherence times are expected in Si QDs owing to the almost spin-zero nuclear background and small spin–orbit interactions. However, fabricating Si QDs small enough to display quantum confinement effects has been difficult because the effective mass for Si is much larger than that for GaAs. The required diameter is ~10 nm or below. Owing to their potential to overcome the obstacle of fabricating such a small Si QD, nanocrystalline Si QDs (nc-Si QDs) have attracted a great deal of attention.[12–14] The nc-Si QDs are promising for developing various applications such as single-electron transistors,[15] light emitting devices,[16] electron emitters,[17] and solar cells[18–21] because of their unique properties, which are affected by quantum confinement. To make use of these interesting properties, it is necessary to understand the electronic states in a single nc-Si QD.

The nc-Si QDs have been fabricated via the decomposition of silane (SiH_4) molecules with very high frequency (VHF; 144 MHz) plasma.[17,22] It is known that increasing the surface oxidation time, shortening the pulse duration of the SiH_4 gas, increasing the VHF plasma power, and increasing the flow rate of the SiH_4 gas supplied into the VHF plasma are all effective methods to reduce the size of nc-Si QDs.[23–26] The transport properties of multiple nc-Si QDs between electrodes have also been studied, which have revealed that quantum confinement enables the nc-Si QDs to transport their carriers through hopping conduction.[12–14] In an attempt to measure transport through a few nc-Si QDs, we previously prepared nanogap (15 nm) electrode devices and virtually observed the characteristics of a single dot over a limited temperature range.[15] However, we could not avoid interference from surrounding QDs.

In this study, we experimentally observed electron transport through a single nc-Si QD between the nanogap electrodes. We developed a fabrication technique for doped silicon electrodes with a 10 nm gap by finely controlling the dose during electron beam lithography (EBL) and controlling the dry etching conditions. We obtained a single nc-Si QD device by depositing nc-Si QDs directly into the ~10 nm gap using a VHF plasma cell. We observed the device's Coulomb diamond at 4.5 K and found that the diamond size depended on the number of electrons. We estimated the charging energy and capacitances from the diamond, which were in good agreement with the values calculated from the size of the nc-Si QD. The magnetic field dependence of the electronic states in a single nc-Si QD was also studied, which is important for the application of the single nc-Si QD to spin-related quantum information devices. From the magnetic field dependence of the Coulomb diamonds, the orbital energy evolution as well as the Zeeman splitting in a single nc-Si QD is discussed.

A schematic image of our device is shown in Figure 1(a). The nano gap electrodes were fabricated using silicon-on-insulator (SOI) substrate with an initial SOI thickness of 100 nm and a buried-oxide (BOX) thickness of 200 nm. The SOI thickness was reduced to 50 nm by thermal oxidation followed by a thinning process with wet etching. Then, the SOI layer was doped via ion implantation and drive-in at 1000 °C for 20 min. The doping concentration was 10^{-19} cm^{-3}. After that, the thermal oxide was removed by wet etching.

The positive resist ZEP-A was coated onto the SOI layer, and the nanogap electrode was patterned using high-resolution EBL. The computer-aided design (CAD) design of the nanogap between the two electrodes was 10 nm. To fabricate a narrow gap, we correctly controlled the EBL dose amount. For example, the dose amount for the nanogap part was larger (420 μC/cm^2) than that for other parts (360 μC/cm^2). After EBL, the pattern was etched using reactive ion etching. To etch SOI vertically, we used Cl_2 gas as the etching gas. Figure 1(b) shows the scanning electron microscope (SEM) image of the etched SOI layer. The gap width was ~9 nm, which is almost the same size as that of the CAD design. Then, we evaporated Al for the contact pads. After that, we checked the electrical isolation of the gap between

[a]Author to whom correspondence should be addressed. Electronic mail: kodera.t.ac@m.titech.ac.jp
[b]soda@pe.titech.ac.jp

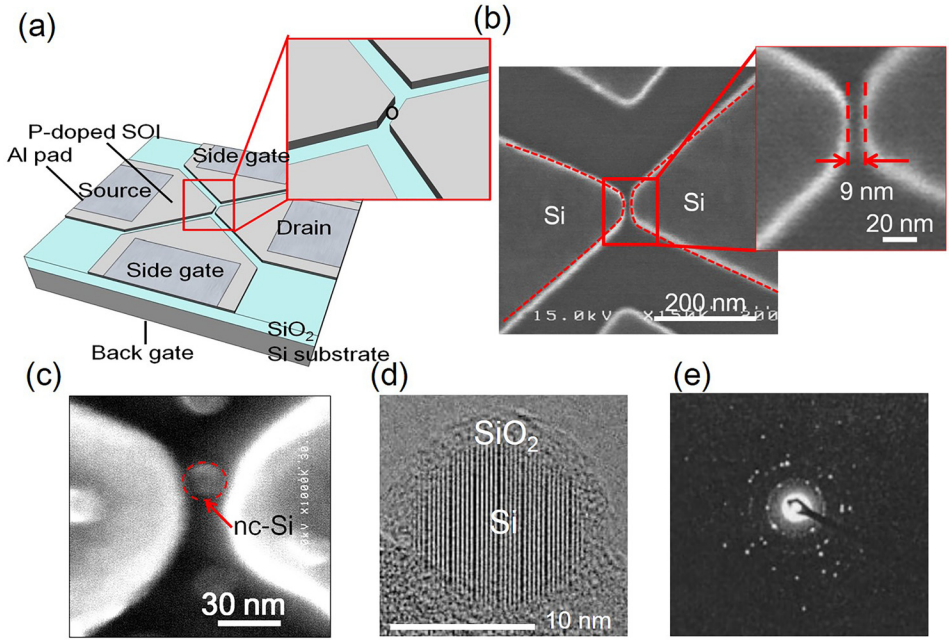

FIG. 1. (a) Schematic image of the device structure. A highly-doped SOI wafer was used as the side gate and for the nanogap electrodes. The doping concentration was on the order of 10^{-19} cm^{-3}. (b) Scanning electron microscope (SEM) image of the nanogap electrodes. The size of the gap was 9 nm. (c) SEM image of the single nanocrystalline silicon quantum dot (nc-Si QD) between the nanogap electrodes. (d) Transmission electron microscope (TEM) image of the nc-Si QD. (e) Electron diffraction pattern of the nc-Si QD.

the two electrodes using an electric prober system since it is important to check the isolation before deposition of the nc-Si QDs.

Finally, we deposited the nc-Si QDs directly on the nanogap electrode. The fabrication equipment for the nc-Si QDs consisted of a VHF plasma cell and an ultrahigh-vacuum chamber. The nc-Si QDs with a diameter of ~10 nm were formed in the gas phase of an SiH_4 plasma cell by decomposing the pulsed SiH_4 gas supplied by the VHF plasma and deposited on the nanogap electrode. Figure 1(c) is an SEM image of our device. A single nc-Si QD was deposited between the nanogap electrodes. Note that two other QDs above and below the center QD are not in contact with the source and drain electrodes, so it is impossible to exchange electrons between the QDs and electrodes. This means these two QDs will not affect the transport measurement results shown hereafter. Figures 1(d) and 1(e) show a transmission electron microscope (TEM) image and an electron diffraction pattern of the nc-Si QDs, fabricated using the same VHF plasma technique, respectively. The parallel lines of the Si region in Fig. 1(d) and the spot patterns in Fig. 1(e) reflect the high crystalline.

We performed electrical measurements to characterize the nc-Si QD. Figure 2(a) shows the comparison of the drain currents I_d before and after deposition of the nc-Si QD measured at 300 K. No current flows without an nc-Si QD in the gap. Conversely, current flows after the deposition of a single nc-Si QD in the gap. This is clearly evident that the nc-Si QD was deposited between the nanogap electrodes and electrically connected to both electrodes. Figure 2(b) shows the drain current I_d as a function of the back gate voltage measured at a temperature of 4.5 K. In this measurement, the drain voltage was 5 mV and side gate voltage was 0 V. We clearly observed the Coulomb oscillation peaks of the single nc-Si QD. Figure 2(c) shows the counter plot of the drain current I_d in the plane of the back gate voltage and drain voltage measured at 4.5 K. The Coulomb diamond characteristics of the single QD were observed. Inside the diamond, the number of electrons on the QD, N, is fixed and transport through the QD is blocked. We found that the size of the diamond indicated by N and $N-2$ is smaller than that of $N+1$ and $N-1$, respectively. This result indicates that the electron number of the large diamond ($N+1$ and $N-1$) is even and the filling of electrons into spin-degenerate single-particle states occurs in the single nc-Si QD. While the addition energy to an N (odd) electron QD is determined by the charging energy, that to an $N-1$ (even) electron QD is determined by the charging energy plus the orbital level spacing. Figure 2(d) shows the magnified plot of the dotted square region in Figure 2(c). From the size of the Coulomb diamond shown in Figure 2(d), the charging energy E_C was estimated to be 11 meV according to $e\Delta V_{sd}$, while the total capacitance C was 15 aF according to e^2/E_C, and the back gate capacitance C_g was 0.07 aF according to $CE_C/e\Delta V_g$. We calculated C_g and C to confirm the validity of the experimentally estimated values with a simplified geometric model. C_g was calculated using the equation $C_g \approx \frac{\varepsilon_{ox}\varepsilon_0}{d}S$, where d is the thickness of the BOX layer (~200 nm), ε_{OX} is the dielectric constant of SiO_2 (~3.9), and S is the contact area between the nc-Si QD and the BOX layer (~10^{-16} m^2), assuming the contact shape is a disk with diameter 10 nm. Thus, C_g was ~0.02 aF, which is a similar value to the capacitance estimated from the measurement results. Next, we calculated the self-capacitance of the nc-Si QD, C_{self}, and the capacitance between the QD and the source/drain electrode, C_{sd}. The shape of our QD was almost that of a perfect sphere; thus, C_{self} was calculated to be ~7 aF using the following equation: $C_{self} \approx 2\pi\varepsilon_{Si}\varepsilon_0 d_{QD}$, where d_{QD} is the diameter of the nc-Si QD (~10 nm) and ε_{Si} is the dielectric constant of Si (~12). C_{sd} can be calculated as follows: $C_{sd} \approx \frac{\varepsilon_{Si}\varepsilon_0\pi d_{QD}^2}{2d_{OX}}$ ~8 aF, where d_{OX} is the thickness of the natural oxide of the nano gap electrode ($d_{OX} \approx 2$ nm). The total capacitance C_{total} ($=C_{self}+C_{sd}+C_g$) is then calculated to be ~15 aF. This value is consistent with C (~15 aF), which was estimated from the measured Coulomb diamond; this therefore

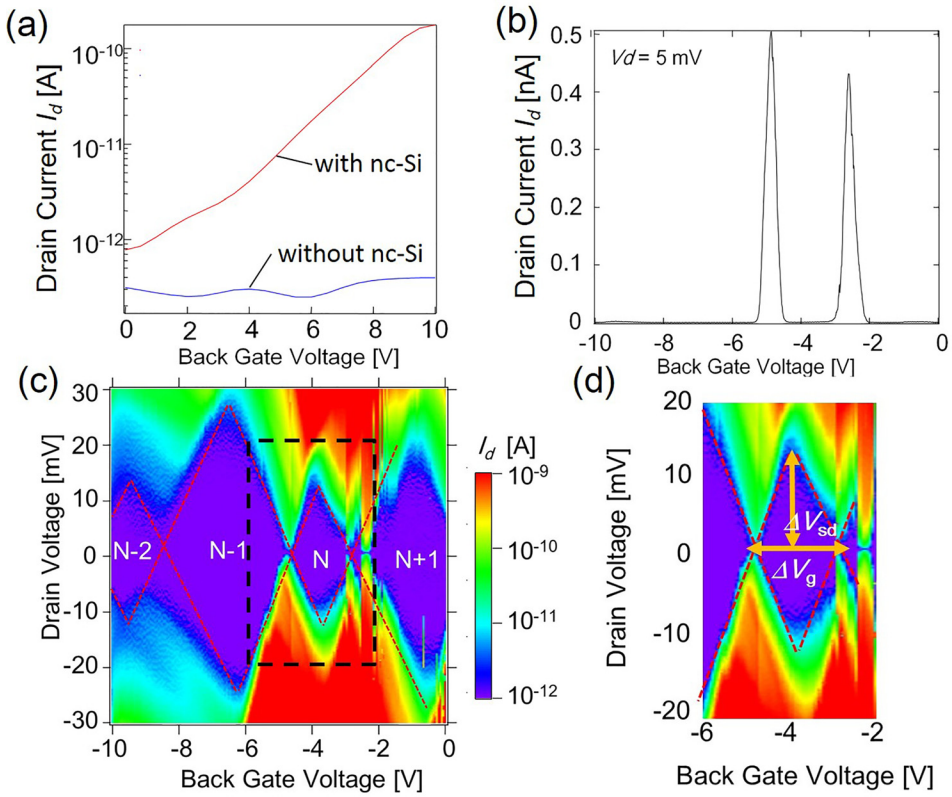

FIG. 2. (a) Comparison of the electric device characteristics with and without nc-Si deposition, measured at room temperature. (b) Coulomb oscillation as a function of back gate voltage measured at 4.5 K. The drain voltage (V_d) was 5 mV. (c) Coulomb diamond characteristics measured at 4.5 K. Different diamond sizes were observed because of shell-filling. (d) Magnified plot of dashed rectangular area shown in (c).

validates that the device fabrication of the single nc-Si QD in the gap was as expected. Note that the relatively large charging energy of 11 meV was observed in the measurements, due to the fact that we achieved the small QD by using the VHF plasma technique.

Figure 3(a) shows the perpendicular magnetic field dependence of the Coulomb peak position measured at 4.5 K, from 0 to 8 T. The data hereafter are taken with a different cooling history from the above mentioned data for Figure 2. The positions of the Coulomb peaks are shifted because electron charging and releasing to/from defects are affected by the history of cooling and heating. At zero magnetic field, we observe Coulomb peaks at −6.4 V (peak 1), −4.9 V (peak 2), −2.6 V (peak 3), and −0.6 V (peak 4). Peaks 1–4 shift with increasing magnetic field. We found that peak 1 shifted slightly toward more negative voltages, while peak 2 remained at almost the same position and peaks 3 and 4 exhibited positive shifts as the magnetic field increased. The trend lines are indicated by dashed arrows. To observe this effect more clearly, we plotted the three successive Coulomb peak spacings against the magnetic field, as shown in Figure 3(b). The trend lines are indicated by dashed arrows. The energy spacings were calculated using the gate capacitance C_g. From the evolution of successive Coulomb peak spacings in the perpendicular magnetic field, we could determine the effect of the Zeeman splitting and the orbital energy evolution. The spacings between peak 1 and peak 2 (indicated by open circles) and between peak 3 and peak 4 (indicated by open triangles) increased with the magnetic field. The slopes obtained by curve fittings for "peak 2–peak 1" and "peak 4–peak 3" are 0.04 and 0.03, respectively. The slopes of the spacing curves are similar to that of 0.03 for the Zeeman energy (indicated by a dotted line) when a g-factor is equal to 2, which is reasonable for Si. Conversely, the spacing between peak 2 and peak 3 (indicated by open squares) increased at a higher rate than the Zeeman energy. The slope obtained by a curve fitting for "peak 3–peak 2" is 0.08. This behavior can be explained by considering the electronic states with respect to their spins and orbitals;[27,28] the electronic states related to peaks 1 (3) and 2 (4) are in the same orbital but have different spin orientations. The electronic states related to peak 2 and 3 are in the different orbitals. The energy difference between the two orbitals increased with increasing perpendicular magnetic field. In order to explain the results that the spacing between peak 2 and 3 increased at a greater rate than the Zeeman energy, the increase should be more than twice the Zeeman energy splitting. This is consistent with the measured increase of the orbital separation of ∼0.1, while the Zeeman energy splitting is 0.03.

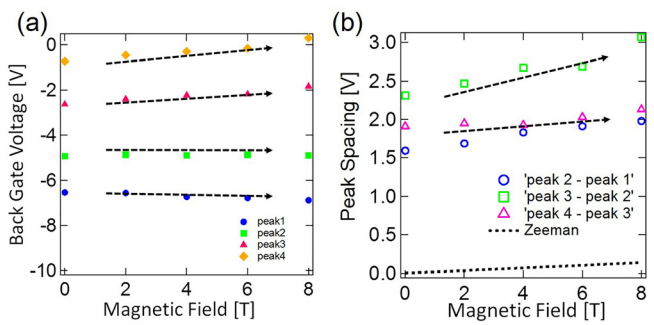

FIG. 3. (a) Perpendicular magnetic field dependence of the Coulomb peak positions. The trend lines are indicated by dashed arrows. (b) Coulomb peak spacings as a function of magnetic field. The Zeeman energy splitting is indicated by a dotted line for a g-factor of 2. The trend lines are indicated by dashed arrows.

In conclusion, we have fabricated a single silicon nanocrystal between the nanogap electrodes and studied its electronic states. We observed the Coulomb diamond at 4.5 K and its size depended on the number of electrons according to even–odd shell filling. The charging energy was estimated to be ~11 meV, which is consistent with the size of the silicon nanocrystal. The perpendicular magnetic field dependence of the Coulomb peaks displayed the Zeeman splitting as well as orbital energy evolution.

Part of this work was financially supported by the Kakenhi Grants-in-Aid (Nos. 26709023 and 26249048) and the Project for Developing Innovation Systems of the Ministry of Education, Culture, Sports, Science and Technology (MEXT) of Japan. The devices were fabricated using facilities of the Nanotechnology Platform at QNERC.

[1]D. Loss and D. P. DiVincenzo, Phys. Rev. A **57**, 120 (1998).
[2]A. Morello, J. J. Pla, F. A. Zwanenburg, K. W. Chan, K. Y. Tan, H. Hueb, M. Mottonen, C. D. Nugroho, C. Yang, J. A. van Donkelaar, A. D. C. Alves, D. N. Jamieson, C. C. Escott, L. C. L. Hollenberg, R. G. Clark, and A. S. Dzurak, Nature **467**, 687 (2010).
[3]B. M. Maune, M. G. Borselli, B. Huang, T. D. Ladd, P. W. Deelman, K. S. Holabird, A. A. Kiselev, I. Alvarado-Rodriguez, R. S. Ross, A. E. Schmitz, M. Sokolich, C. A. Watson, M. F. Gyure, and A. T. Hunter, Nature **481**, 344 (2012).
[4]E. Kawakami, P. Scarlino, D. R. Ward, F. R. Braakman, D. E. Savage, M. G. Lagally, M. Friesen, S. N. Coppersmith, M. A. Eriksson, and L. M. K. Vandersypen, Nat. Nanotechnol. **9**, 666 (2014).
[5]D. Kim, Z. Shi, C. B. Simmons, D. R. Ward, J. R. Prance, T. S. Koh, J. K. Gamble, D. E. Savage, M. G. Lagally, M. Friesen, S. N. Coppersmith, and M. A. Eriksson, Nature **511**, 70 (2014).
[6]M. Veldhorst, C. H. Yang, J. C. C. Hwang, W. Huang, J. P. Dehollain, J. T. Muhonen, S. Simmons, A. Lauch, F. E. Hudson, K. M. Itoh, A. Morello, and A. S. Dzurak, Nature **526**, 410 (2015).
[7]X. Hao, R. Ruskov, M. Xiao, C. Tahan, and H. Jiang, Nat. Commun. **5**, 3860 (2014).
[8]M. Veldhorst, J. C. C. Hwang, C. H. Yang, A. W. Leenstra, B. de Ronde, J. P. Dehollain, J. T. Muhonen, F. E. Hudson, K. M. Itoh, A. Morello, and A. S. Dzurak, Nat. Nanotechnol. **9**, 981 (2014).
[9]K. Horibe, T. Kodera, and S. Oda, Appl. Phys. Lett. **106**, 083111 (2015).
[10]G. Yamahata, T. Kodera, H. O. H. Churchill, K. Uchida, C. M. Marcus, and S. Oda, Phys. Rev. B **86**, 115322 (2012).
[11]S. Ihara, A. Andreev, D. A. Williams, T. Kodera, and S. Oda, Appl. Phys. Lett. **107**, 013102 (2015).
[12]M. A. Rafiq, Y. Tsuchiya, H. Mizuta, S. Oda, S. Uno, Z. A. K. Durrani, and W. I. Miline, Appl. Phys. Lett. **87**, 182101 (2005).
[13]M. A. Rafiq, Y. Tsuchiya, H. Mizuta, S. Oda, S. Uno, Z. A. K. Durrani, and W. I. Miline, J. Appl. Phys. **100**, 014303 (2006).
[14]X. Zhou, K. Usami, M. A. Rafiq, Y. Tsuchiya, H. Mizuta, and S. Oda, J. Appl. Phys. **104**, 024518 (2008).
[15]A. Dutta, S. Oda, Y. Fu, and M. Willander, Jpn. J. Appl. Phys. **39**, 4647 (2000).
[16]H. J. Cheong, A. Tanaka, D. Hippo, K. Usami, Y. Tsuchiya, H. Mizuta, and S. Oda, Jpn. J. Appl. Phys. **47**, 8137 (2008).
[17]K. Nishiguchi, X. Zhao, and S. Oda, J. Appl. Phys. **92**, 2748 (2002).
[18]Y. Kurokawa, S. Tomita, S. Miyajima, A. Yamada, and M. Konagai, Jpn. J. Appl. Phys. **46**, L833 (2007).
[19]J. M. Luther, M. Law, M. C. Beard, Q. Song, M. O. Reese, R. J. Ellingson, and A. J. Nozik, Nano Lett. **8**, 3488 (2008).
[20]C. Liu, Z. C. Holman, and U. R. Kortshagen, Nano Lett. **9**, 449 (2009).
[21]V. Svrcek, I. Turkvych, and M. Kondo, Nanoscale Res. Lett. **4**, 1389 (2009).
[22]T. Ifuku, M. Otobe, A. Itoh, and S. Oda, Jpn. J. Appl. Phys. **36**, 4031 (1997).
[23]Y. Kanemitsu, S. Okamoto, M. Otobe, and S. Oda, Phys. Rev. B **55**, R7375 (1997).
[24]K. Nishiguchi, S. Hara, T. Amano, S. Hatatani, and S. Oda, Mater. Res. Soc. Symp. Proc. **571**, 43 (1999).
[25]Y. Nakamine, N. Inaba, T. Kodera, K. Uchida, R. N. Pereira, A. R. Stegner, M. S. Brandt, M. Stutzman, and S. Oda, Jpn. J. Appl. Phys. **50**, 025002 (2011).
[26]K. Someno, K. Usami, T. Kodera, Y. Kawano, M. Hatano, and S. Oda, Jpn. J. Appl. Phys. **51**, 115202 (2012).
[27]L. P. Kouwenhoven, D. G. Austing, and S. Tarucha, Rep. Prog. Phys. **64**, 701 (2001).
[28]R. Hanson, L. P. Kouwenhoven, J. R. Petta, S. Tarucha, and L. M. K. Vandersypen, Rev. Mod. Phys. **79**, 1217 (2007).